Phase-matching effects in strong-field harmonic generation

Ph. Balcou and Anne L'Huillier
Service des Photons, Atomes et Molécules, Bâtiment 522, Centre d'Etudes de Saclay, 91191 Gif-sur-Yvette, France
(Received 20 August 1992)

We present experimental results of harmonic generation at 1064 nm using a 36-ps neodymium-doped yttrium aluminum garnet laser tightly focused in a gas jet of xenon. The harmonic yields are studied as a function of the position of the focus in the jet at several laser intensities and as a function of intensity at several focus positions. These results bring information about how the high harmonics are phase matched in the medium and also about the single-atom dynamics of the process. The harmonic yields as a function of the position of the focus in the jet exhibit regular oscillations that are due to the interference effects inherent to the generation of harmonics in the nonlinear medium. The intensity dependences present structures that we attribute to single-atom resonance effects.
PACS number(s) : 42.65 Ky, 32.80 Rm

I. INTRODUCTION

High-order harmonic generation by atoms in intense laser fields has recently drawn considerable attention. Experiments [1–6] have demonstrated the possibility to reach wavelengths shorter than 20 nm with reasonable conversion efficiencies, thus opening the way to the development of high brightness coherent sources in the vacuum ultraviolet (VUV) and soft x-ray ranges. These conversion processes depend on the interplay between the single-atom response to the external laser field and macroscopic phase-matching effects. It is essential to understand both aspects in order to optimize the number of photons that can be produced.

Phase-matching effects have been extensively studied in the case of low-order processes in cells [7]. There are essentially two reasons for phases not to be matched: the *dispersion* in the nonlinear medium which induces a phase difference between the polarization and the generated field and the *focusing* of the laser beam which also leads to an effective phase mismatch [8]. The effect of dispersion increases with the atomic density and is very sensitive to the presence of resonances. In contrast, the effect due to focusing is purely geometrical. Thus, a well-known result is that no harmonics can be created when a laser is focused in a positively dispersive infinite medium. The situation becomes more complicated when harmonics are generated in thin gas jets [9, 10]. This introduces another length, the medium length, which can be comparable to the laser confocal parameter. Moreover, one has to take into account a nonuniform atomic density and in particular edge effects. Harmonic generation in a jet has been carefully studied by Lago *et al.* [11, 12], who have investigated in particular the influence of the position of the beam focus in the gas jet on third harmonic generation, considering several analytical distributions for describing the atomic density. The cancellation of the harmonic fields in a positively dispersive finite medium is not perfect. It depends on the ratio between the length of the jet (L) and the laser confocal parameter (b) and increases dramatically with the process order [13].

Most of the above studies (and in particular those performed with a gas jet) need relatively weak laser intensities (below 10^{12} W/cm^2), so that the atomic response can be treated within lowest-order perturbation theory. In this weak-field limit, the polarization of the medium induced by the laser field at the qth harmonic frequency $q\omega$ is simply expressed as $\chi^{(q)}E^q$, the product of a nonlinear susceptibility by the qth power of the field strength. As the laser intensity reaches values of the order of 10^{13} W/cm^2 or more, which are necessary to generate the high-order harmonics, the atomic response departs largely from that predicted by lowest-order perturbation theory. The atom becomes strongly perturbed by the radiation field. Single-atom studies of harmonic intensity dependences [14] show that the dynamics of these processes look indeed very complicated, with many structures and resonances (the ionization rate being in contrast much smoother). However, the harmonic intensity distribution at a given laser intensity is quite simple and exhibits a characteristic universal shape. It decreases for the first orders, then is almost constant over a wide range of photon energies, and finally decreases rapidly. This behavior has been reproduced in most single-atom calculations [15–18] and also in more complete studies including propagation of the harmonic fields in the nonlinear medium (phase matching) [19, 20]. In contrast to the perturbative result mentioned above, phase matching turns out to remain almost constant for the harmonics in the plateau region. This comes from the fact that in this strong-field regime, all of the plateau harmonics vary similarly with the laser intensity and much more slowly than in the weak-field limit. Moreover, the propagation was found to be mostly governed by an effective phase mismatch, due to the beam focusing. When the atomic dipole moment at the har-

monic frequency $q\omega$ is assumed to vary as the pth power of the laser field, p being an effective order of nonlinearity smaller than q, the harmonic field displays interference fringes within the medium, separated by twice a coherence length $L_{\rm coh} = b\tan[\pi/(q-1)]/2$ [20, 21]. These fringes are similar to those displayed by a harmonic field generated in nonlinear dispersive media, which can be probed for instance by rotating a crystal plate (Maker fringes [22]), or by varying the atomic density in the case of a gas target [23]. However, their origin is geometrical: they can be probed by varying the interaction geometry, or the focusing conditions. Moreover, their observation requires that the polarization induced by the fundamental field varies slowly in the nonlinear medium, and henceforth departs from the perturbative limit.

In this work, we present experimental studies of these phase-matching effects induced by focusing, which are the signature of the nonperturbative response of atoms to strong fields. We have concentrated our effort on xenon, using a 1064-nm, 36-ps, 10-Hz Nd-YAG laser (YAG denotes yttrium aluminum garnet). We get evidence of the fringes by studying the harmonic yields from $q = 3$ to 15 at a given intensity, as a function of the position of the laser focus in the atomic beam. These results, combined with harmonic intensity dependences, also give some insight on the single-atom aspect of the problem. The harmonics in general do not have a smooth dependence with intensity and exhibit structures which we attribute to the influence of resonances [21, 24], most of the single-atom rapidly varying features being, however, averaged out by propagation. Some of our results have been presented recently in a Letter [21]. We give here a full account of these experiments, together with a detailed interpretation.

This article is organized as follows. In Sec. II we summarize the theoretical background needed for discussing the experimental results. In particular, we make the connection between the variations of the harmonic yield when displacing the focus, and the interference fringes within the medium at a given focus position. We present in Sec. III systematic studies of harmonic yields in xenon at 1064 nm, as a function of the laser intensity and of the focus position. The results are discussed in Sec. IV.

II. PHASE MATCHING IN A GAS JET

A. Definition of the coherence length

Consider an incident laser field, with a Gaussian envelope expressed as

$$E_1(r,z) = \frac{E_0}{b+2iz}\exp\left(\frac{-k_1 r^2}{b+2iz}\right), \tag{1}$$

where E_0 is the peak field amplitude and k_1 is the wave vector. The envelope of the nonlinear polarization induced by the laser at frequency $q\omega$ (ω being the laser frequency) can be written as

$$P_q(r,z) = 2\mathcal{N}_0\rho(r,z)d_q(r,z) \times \exp\left[-iq\left(\tan^{-1}(2z/b) - \frac{2k_1 r^2 z}{b^2+4z^2}\right)\right], \tag{2}$$

where $\mathcal{N}_0$ and $\rho(z)$ are the peak density and density profile of the jet, and d_q is the complex dipole moment, such that $d_q e^{iq(\omega t+\phi)}$ is the component oscillating at $q\omega$ of the atomic response to the electric field $|E_1|e^{i(\omega t+\phi)}$. The space-dependent phase ϕ induced by the laser beam focusing leads to the phase factor in Eq. (2). For a dispersionless medium (such that the phase mismatch Δk is zero), the phase lag between $P_q(z)$ and a freely propagating Gaussian beam at $q\omega$ is

$$\Delta\phi(z) = (1-q)\tan^{-1}(2z/b). \tag{3}$$

This phase lag can be interpreted as the absolute phase of a Gaussian beam at $q\omega$ generated by a slab of polarization between z and $z+\delta z$:

$$\delta E_q^{[z,z+\delta z]}(r',z') \sim \frac{\exp[i\Delta\phi(z)]}{1+2iz'/b}\exp\left(\frac{-k_q r'^2}{b+2iz'}\right), \tag{4}$$

whose phase reduces to that of P_q for $z' = z$. The harmonic fields generated by two slabs separated by one coherence length, defined to be $L_{\rm coh} = (b/2)\tan[\pi/(q-1)]$ close to the focus, are dephased by π and hence interferer mostly destructively. This leads to interference fringes in the medium, separated by $2L_{\rm coh}$ [21]. Because of the arctangent function, the distance between two zeros modulo π of $\Delta\phi(z)$ increases away from the focus. To second order in z/b, we have

$$L_{\rm coh}(z) = \frac{\pi b}{2(q-1)}\left(1+\frac{4z^2}{b^2}\right). \tag{5}$$

For a medium with dispersion, the phase lag between the polarization and the free Gaussian beam propagating in the medium is

$$\Delta\phi(z) = (1-q)\tan^{-1}(2z/b) + \Delta k z, \tag{6}$$

where Δk is the phase mismatch $k_q - qk_1$.

As discussed in previous work [19, 20], phase matching of focused beams depends not only on the effective phase mismatch (or coherence length) but also on how the amplitude of the polarization varies throughout the medium. If the length over which the polarization is concentrated (denoted $L_{\rm amp}$) is comparable to or smaller than L, the number of interference fringes that can develop in the nonlinear medium will be given by $L_{\rm amp}/2L_{\rm coh}$ rather than $L/2L_{\rm coh}$. This explains the difference between phase matching in a weak- or strong-field regime for the laser-atom interaction. In a weak-field regime, the nonlinear polarization for a high harmonic is quite concentrated in the medium, $L_{\rm amp} \approx 2L_{\rm coh} \ll L$ and only one fringe appears. The field grows, reaches a maximum close to the focus, and then decreases. The field created over the first half of the medium is cancelled out by that created in the second half. In contrast, in a strong-field regime, $L_{\rm amp}$ is much larger and several fringes appear. The cancellation does not occur. As a result, phase matching of the high harmonics is considerably enhanced in a strong-field regime as compared to the perturbative limit.

So far, we have considered harmonic generation when the laser is focused at the center of the atomic beam. It

is important to understand the effect of the displacement of the focus relative to the center of the medium on phase matching both in strong- or weak-field limit situations. Indeed, by studying phase matching as a function of the position of the focus in the jet, we probe not only the interference effects mentioned above but also the density distribution in the beam (and its edges). We first consider the weak-field limit, for which analytical expressions can be given [11]. In the following, we neglect dispersion, whose effect remains small compared to that of focusing in our experimental conditions.

B. Calculations within lowest-order perturbation theory

Let Z denote the position of the focus and $Z = 0$ the position of the center of the atomic jet. The incident beam focused at Z is $E_{1,Z}(r,z) = E_0 G^{\omega}_{b,Z}(r,z)$, where $G^{\omega}_{b,Z}$ is the translated Gaussian envelope function obtained from Eq. (1) by replacing z by $z - Z$. The harmonic field generated in the medium is given by

$$E_{q,Z}(r,z) = -i\pi k_q b \mathcal{N}_0 2^{1-q} \chi^{(q)} E_0{}^q G^{q\omega}_{b,Z}(r,z) F_q(Z), \tag{7}$$

where $F_q(Z)$ is the dimensionless phase-matching factor defined by

$$F_q(Z) = \int_{-\infty}^{+\infty} [1 + 2i(z-Z)/b]^{1-q} \rho(z) 2\, dz/b. \tag{8}$$

$F_q(Z)$ can be determined analytically for a Lorentzian density distribution, $\rho(z) = 1/(1 + 4z^2/L^2)$,

$$F_q^{\mathrm{Lor}}(Z) = \frac{\pi b^{q-2}}{(b + L + 2iZ)^{q-1}}, \tag{9}$$

and for a square distribution: $\rho(z) = 1$ if $|Z| < L/2$,

$$F_q^{\mathrm{sq}}(Z) = \frac{-ib^{q-2}}{2-q} \left\{ \frac{1}{[b + 2i(-Z + L/2)]^{q-2}} - \frac{1}{[b + 2i(-Z - L/2)]^{q-2}} \right\}. \tag{10}$$

Figure 1 shows $|F_q(Z)|^2$, $q = 3, 7, 21$ for a Lorentzian (dashed line) and square (solid line) jet density. We use the experimental parameters both for the laser confocal parameter, $b = 1.5$ mm, and for the width of the gas jet, $L = 1$ mm. In the Lorentzian case, all of the curves present a single maximum at $Z = 0$. In contrast, the curves obtained by assuming a square jet exhibit a double-peak structure from the seventh harmonic, the maxima being centered on the medium's edges. The width of the peaks, related to the length L_{amp}, decreases when the harmonic order q increases. Phase matching is considerably enhanced when the laser is focused on one of the edges [see in particular Fig. 1(c)]. Indeed, in the perturbative regime, and for a high-order harmonic, the polarization is mostly concentrated in a region much smaller than that defined by the gas jet. If the atomic density is smooth, the harmonic field will be very similar to the one that would be generated in a large uniform medium [7], i.e.,

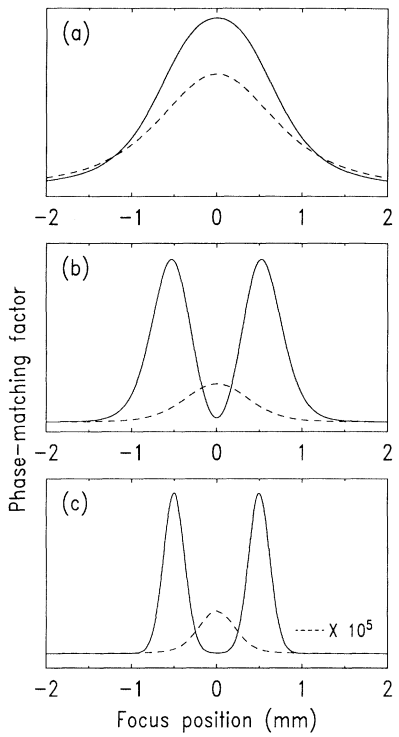

FIG. 1. Phase-matching function $F_q(Z)$ for the 3rd (a), 7th (b), and 21st (c) harmonics in lowest-order perturbation theory, for a 1-mm-wide square (solid line), and Lorentzian (dashed line) jet profile. The confocal parameter is equal to 1.5 mm. The result obtained for the 21st harmonic with the Lorentzian jet has been multiplied by a factor of 10^5.

almost equal to zero. The harmonic field generated on one side of the focus interferes destructively with that generated on the other side. In the case of a square jet, this cancellation does not take place when the focus is located on one of the edges of the medium.

We have performed calculations using more complex density distributions, for which no analytical expression for $F_q(Z)$ can be given. Our conclusion is that for the high harmonics in a perturbative regime, phase matching is very sensitive to any change of slope of the density profile. This is because the perturbative phase-matching factor for the high harmonics is extremely small, and can be improved easily by any irregularity in the shape of the jet. This sensitivity is bound to be much reduced for more realistic harmonics whose phase matching is enhanced by nonperturbative effects [19].

C. Study of a model polarization law

We now investigate how the phase-matching dependence with Z (Fig. 1) is modified when the polarization field does not vary as the qth power of the incident field. Here, for illustration purposes, we use model polarization fields, varying as the pth power of the field, with $p = 4 \ll q$. We show in Fig. 2 $F_q(Z)$ for the 7th, 9th, and 13th harmonics. The solid line and dashed line cor-

respond to results obtained by neglecting dispersion for 1-mm-width square and Lorentzian profiles, respectively. The result shown as a dot-dashed line has been obtained also for a square profile, but with introduction of a phase mismatch due to dispersion, and for the case of the 13th harmonic an absorption factor (we use realistic values, from Ref. [13]). Note that, in all these examples, we cannot find analytical expressions for the phase-matching factor $F_q(Z)$. This factor is determined by solving numerically the propagation equation for the harmonic field in the medium, in the paraxial and slowly varying envelope approximations [20]. The results are quite different from those in Fig. 1. Oscillations appear that cannot be attributed to any density variation (edges), but rather to the interference effects mentioned above. Note that these oscillations strongly depend on the type of density profile used. We now consider in more details the relationship between these oscillations and the coherence length of harmonic generation.

Consider first a semi-infinite medium (from $-\infty$ to $L/2$). Moving the focus Z in this medium is equivalent to varying the position of its right edge (at $L/2$). The oscillations observed in the harmonic yield as a function of the focus are directly related to the interference fringes which appear in the building up of the harmonic field in the medium and the distance between two maxima is twice the coherence length $L_{\mathrm{coh}}(Z)$ [see Eq. (5)].

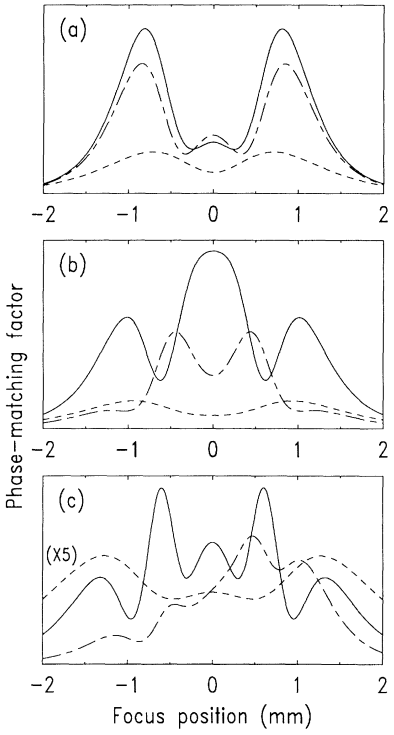

FIG. 2. Phase-matching function $F_q(Z)$ for the 7th (a), 9th (b), and 13th (c) harmonics, for a model $|E|^4$ polarization field and a 1-mm square (solid line) or Lorentzian (dashed line) density profile. The dot-dashed curve corresponds to the square profile case, in which we also consider an atomic phase mismatch, whose real part is positive. The Lorentzian curve in (c) has been multiplied by 5.

When $2L_{\mathrm{coh}} < L_{\mathrm{amp}} < L$, a condition which depends on the variation with intensity of the polarization and on the focusing geometry, the whole interference figure is essentially the same as for a semi-infinite medium. Consequently, moving the focus position is equivalent to spanning the interference fringes directly within the medium. In a tight focusing geometry, we therefore expect the oscillations to follow the coherence length.

Let us now consider a weaker focusing geometry (or a slower variation of the polarization with intensity) such that $2L_{\mathrm{coh}} < L < L_{\mathrm{amp}}$. The semi-infinite medium approximation is no longer valid and the number of oscillations in the curves obtained by moving the focus in the jet does not correspond to the number of interferences expected in the medium when the focus is at $Z = 0$. The number of fringes $n(Z)$ that may develop in the medium when the focus is at position Z is equal, for a square density, to

$$n(Z) = \frac{(q-1)}{2\pi}\left\{\tan^{-1}[(2Z+L)/b] - \tan^{-1}[(2Z-L)/b]\right\}. \tag{11}$$

As Z describes the arctangent curve, $n(Z)$ increases from zero to a maximum integer value (for $Z = 0$) and then decreases again to zero. The harmonic conversion is maximum when $n(Z)$ takes an integer value and minimum when $n(Z)$ is half-integer. Therefore, the harmonic conversion as a function of the position of the focus in the jet exhibits oscillations, with a period approximately equal to $2bL_{\mathrm{coh}}/L$. The transition between the two regimes happens when $L_{\mathrm{amp}} \approx L$.

Finally, if $L < 2L_{\mathrm{coh}}$, almost perfect phase matching is achieved, and no oscillation is observed. This situation corresponds to a very loose focusing geometry, characterized by a linear increase of the observed number of photons with the confocal parameter b, as shown in [4].

Let us now comment in more detail on the results shown in Fig. 2. The periods of the curves corresponding to the square profile (solid line) are close to, or slightly larger than, twice the corresponding coherence lengths. We are in the conditions of validity of the semi-infinite medium approximation discussed above. On the other hand, for the Lorentzian profile, the number of photons always presents only two maxima which correspond to a compromise between the improvement of phase matching, due to the increase of the coherence length away from the focus, and the (slow) decrease of the polarization amplitude. All other oscillations are totally blurred, because of the lack of a well-defined exit edge in the medium, on which interference effects existing in the medium can be probed. Edges, even though they do not lead to a dramatic improvement of phase matching as in the perturbative case, are therefore essential to observe the phase-matching fringes.

In the square jet case, the introduction of a positive phase mismatch, as expected, leads to narrower oscillations, and to a slightly smaller phase-matching factor, as shown by the dot-dashed line in Fig. 2. When the phase

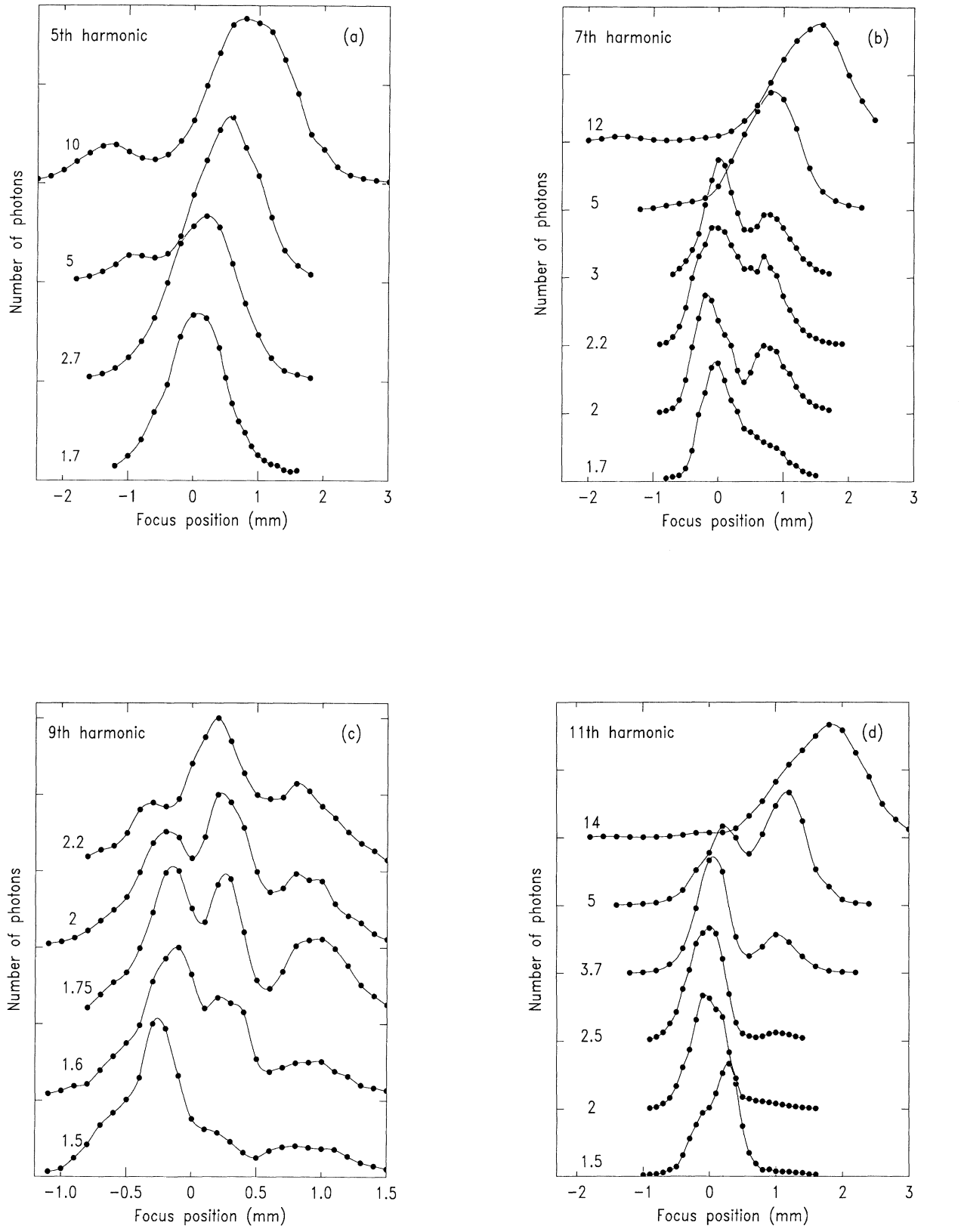

FIG. 3. Number of photons at the 5th harmonic (a), 7th harmonic (b), 9th harmonic (c), 11th harmonic (d), and 13th harmonic below (e) and above (f) the saturation intensity, as a function of the position of the focus in the jet.

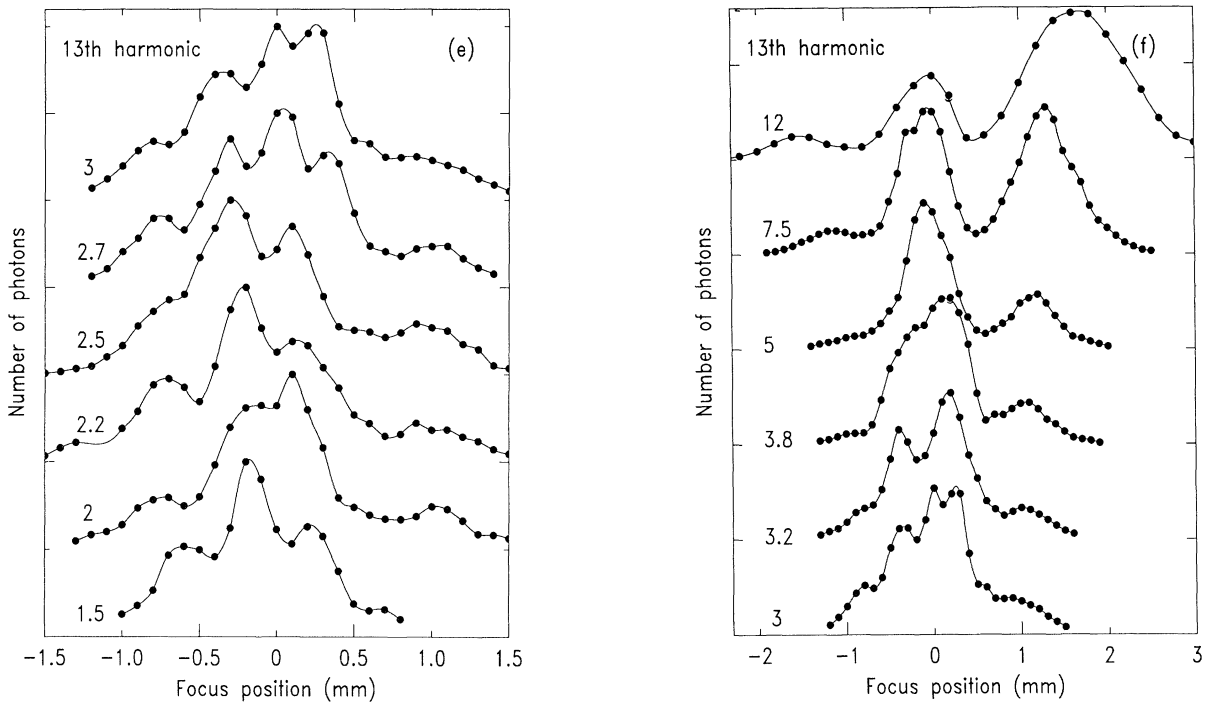

FIG. 3. (*Continued*).

mismatch becomes complex, i.e., when there is some absorption, the curve becomes asymmetric [see Fig. 2(c)].

III. EXPERIMENTAL RESULTS

A. Experimental arrangement

The experimental arrangement has been described elsewhere [2, 3]. We use a mode-locked Nd-YAG laser, delivering 36-ps bandwidth limited pulses, up to 20 mJ in energy. The beam is focused by either a 200-mm or a 300-mm lens in a gas jet of Xe or Ar. We operate the gas jet with a backing pressure of 150 Torr, which yields a 15-Torr peak pressure 0.5 mm below the nozzle. The VUV light is analyzed in the forward direction by a monochromator, consisting of a grazing-incidence gold-coated toroidal grating which refocuses the harmonic light on a 100-μm output slit.

To characterize the focusing geometry, we take successive beam sections in the vicinity of the focus along the propagation axis using a microscope objective (with a magnification of 40) and a charged coupled device camera. The confocal parameter of the beam is given by $b = 4S/\lambda$, where S is the smallest section, or alternatively by measuring the distance between the two sections whose value is $2S$. For the f=200-mm lens, we get S=360 μm^2 and b=1.5 mm; for the f=300-mm lens, S= 750 μm^2, b=3 mm. The intensity range is then 10^{13} to 10^{14} W/cm^2.

The main difficulty in these experiments was first to characterize as well as possible the density profile and second to find the position of the focusing lens for which the focal point was centered in the gas jet. Our method is analogous to that described in [12]. We measure the third harmonic conversion as a function of the jet position relative to the laser focus both perpendicular to and along the propagation axis. Then, we compare the data to theoretical results for the conversion efficiency obtained by assuming various density profiles. The density distribution in the jet looks like a Lorentzian profile with a flat top, with a 1-mm full width at half maximum. The extrema of this top can be considered as "edges," though they are not as clearly defined as for a square profile. This particular shape is due to the short distance between the 6-mm-long nozzle and the laser axis (0.5 mm).

The experiments consist in measuring the harmonic yield as a function of the position of the focus in the jet at various intensities and as a function of intensity at various focus positions. For the first type of measurements, we simply move the focusing lens by steps of 100 μm. We use a large statistic, i.e., 100 laser shots per data point, and we enforce a strict energy selection, with a dispersion of only 5%. For the second type of experiments, we vary the laser energy by rotating a half-wave plate placed before a polarizer (after the last amplifier) and we average the signal over about 30 laser shots. We now discuss the results of these experiments successively.

B. Harmonic generation as a function of the focus position in the jet

We show in Fig. 3 the numbers of photons for the 5th, 7th, 9th, 11th, and 13th harmonics as a function of the

position of the focus in the jet at several laser intensities. The laser propagates from the left to the right. The solid curves are spline interpolations of the data. We use a linear scale in order to emphasize the oscillations. The tick marks on the ordinate scale indicate the zero for each curve. The intensity is printed above the tick marks in units of 10^{13} W/cm^2. The saturation intensity is estimated to be 3×10^{13} W/cm^2. The two or three highest curves in Figs. 3(a), 3(b), and 3(d) and, for the 13th harmonic, all of the curves in Fig. 3(f) have been obtained in the saturation region. We first comment on the results below 3×10^{13} W/cm^2.

The 5th harmonic is the only curve together with the 3rd harmonic [21] which exhibits a single maximum when the best focus is at the center of the jet ($Z = 0$). The 7th harmonic shows two peaks at approximately the same positions ($Z = -0.1$ and $Z = 0.7$) for all of the results below saturation, the 9th harmonic three peaks at $Z = -0.25$, 0.25, and 0.8, and the 13th harmonic about 4 or 5 oscillations separated by about 0.2 mm. The 11th and all of the harmonics higher than the 13th (the highest being the 21st) present a single peak, sometimes with shoulders as shown in Fig. 3(d), always much broader than what is expected from lowest-order perturbation theory. The periods of the oscillations are measured to be 0.8, 0.5, and 0.25 mm for the 7th, 9th, and 13th harmonics, respectively, to be compared to 0.8, 0.6, and 0.4 mm for twice the corresponding coherence lengths due to focusing. They are approximately independent of intensity and they increase slightly away from the center. We interpret these oscillations as the signature of phase-matching effects. The fact that the period is consistent with $2L_{\rm coh}$ implies that we are close to the semi-infinite medium approximation described in the preceding section: the geometry is tight enough for $L_{\rm amp}$ to be smaller than L.

All of the harmonics apart from the 3rd and 5th display a strong asymmetry. In the Appendix, we consider the symmetry properties of these curves as a function of Z and we investigate the different causes for an asymmetry: absorption in the nonlinear medium, nonperturbative response leading to a complex dipole moment, or asymmetric density distributions. Ionization being an 11-photon process (in a weak-field picture), there is absorption in the nonlinear medium for the harmonics of order higher or equal to 11, which leads to asymmetric curves as a function of Z. For the 7th and 9th harmonics, the experimental asymmetry might be due either to a slight defect of our gas jet or to the intrinsic phase of the atomic dipole moment at $q\omega$, arising from a nonperturbative response (see the Appendix), or to an intensity-dependent absorption coefficient.

In contrast to the period of the oscillations, practically independent of intensity, the relative amplitudes of the peaks exhibit dramatic changes with the laser intensity over a small range. For instance, for the 9th harmonic, a central peak, hardly distinguishable at 1.5×10^{13} W/cm^2, appears at 1.6×10^{13} W/cm^2 and becomes dominant around 1.8×10^{13} W/cm^2. Similar behaviors can be observed on the 7th and 13th harmonics in Figs. 3(b) and 3(e); In the latter case, there is even an additional structure appearing between 2.5 and 2.7 $\times 10^{13}$ W/cm^2. These rapid variations in intensity cannot be accounted for by any effective power-law type of polarization fields. They are probably due to resonances, or more generally rapidly varying features, of the single-atom response. Studies of harmonic generation as of function of intensity (see the next section) will bring more information on these features.

The results obtained in the saturation region, above 3×10^{13} W/cm^2, are quite different. Consider, for example, Fig. 3(f). Between 3 and 3.8 $\times 10^{13}$ W/cm^2, the width and shape of the curves do not change much but the fine structure disappears. This is because the phase mismatch gets an additional contribution from the free electrons. It increases with the electron density, and consequently with the laser intensity, thus mixing up the interference pattern due to focusing. Moreover, from about 5×10^{13} W/cm^2, for all of the harmonics, a second and then a third structure, respectively on the right and on the left of the figures, grows and becomes dominant. The number of photons at $Z = 0$ does not decrease in absolute value: it saturates, because the neutral medium gets depleted. However, the intensity is now high enough for harmonics to be generated far from the best focus site. For these large Z values, the coherence length $L_{\rm coh}(Z)$ is much larger than at $Z = 0$ which leads to a more important harmonic production, up to a factor of 50 more [4]. As the intensity increases, the region where the harmonic signal is maximum moves farther away, as shown in Fig. 3(f) for the highest intensity results. Note that the curves exhibit a strong asymmetry, even in the saturation region. It might be due to absorption in the medium, because the structure on the left, which corresponds to the laser being focused at the entrance of the medium, is reduced relative to the one on the right. However, this asymmetry happens to be reversed for the 17th harmonic (and also higher-order ones, as observed recently with a shorter pulse laser [25,26]) which seems to contradict this interpretation.

We now study the intensity dependences of the harmonic yields, for different Z positions.

C. Laser intensity dependence of harmonic conversion

Figure 4 presents on a double logarithmic plot the number of photons as a function of laser intensity for three different focus positions, for the 7th and 13th harmonics. Solid lines are high-order B-spline fits of the experimental points which help in following the curves. We present mostly results obtained when the laser is focused near the exit of the medium, because these are the most interesting, with the richest structure. The behavior of the intensity dependences of each harmonic changes sometimes dramatically when moving from one focus position to another. The result obtained at the seventh harmonic is rather smooth at $Z = 0$ but shows one and two pronounced structures at $Z = 0.4$ and $Z = 0.6$ mm, respectively. This is completely in contradiction with the predictions of perturbation theory, which leads to I^q power laws, independently of the focus position. There

are two intensity regions where abrupt changes of slope are observed for the 7th and 13th harmonics (and this also applies for the 9th and 11th harmonics, not shown here): around 1.5×10^{13} and around 2.5×10^{13} W/cm^2. Note that the 13th harmonic even displays a decrease in harmonic conversion at 1.9×10^{13} W/cm^2 and Z=0.5 mm. Ionization effects become dominant above 3×10^{13} W/cm^2.

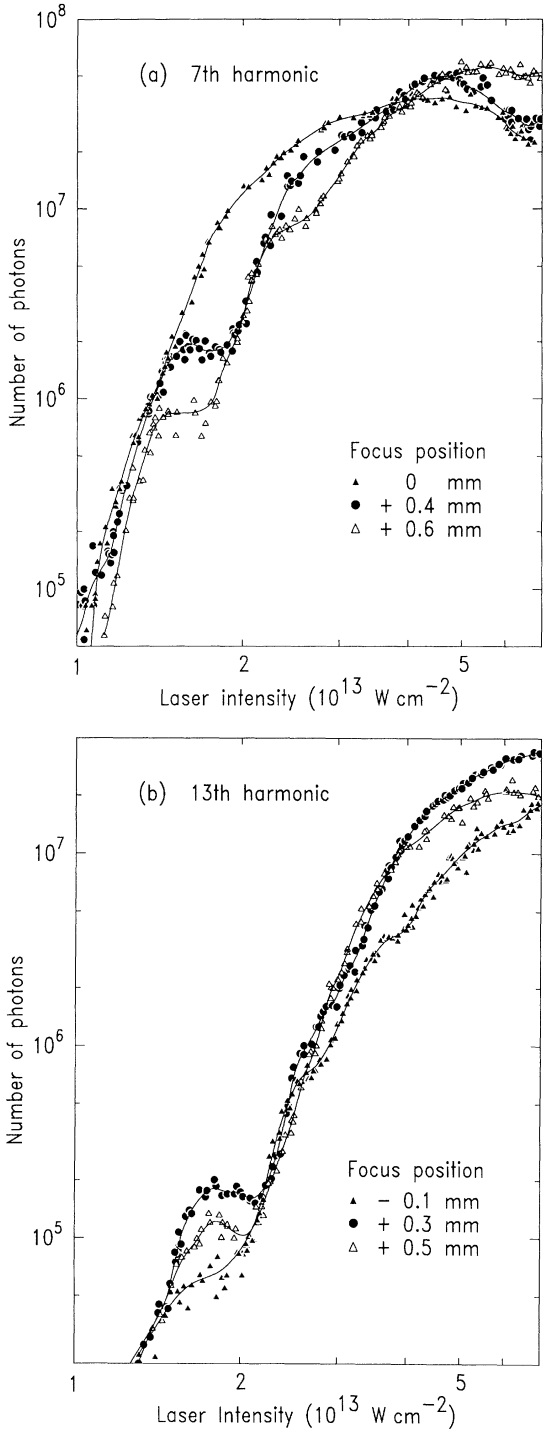

FIG. 4. Number of photons at the 7th (a) and 13th (b) harmonics as a function of the laser intensity.

These structures are probably due to the influence of resonant excited states of the atom, as will be discussed in the next section. Note the strong dependence of the curves on the geometry of the interaction (and in particular on the position of focus). Propagation can average out a structure as is the case when the laser is focused at the entrance of the medium (for which the propagation length is maximum). In contrast, it emphasizes them for positive Z positions (the laser being focused at the exit of the medium). Decreases in harmonic intensity dependences cannot be observed in multiphoton ionization processes because the volume in which resonant processes take place always increases with intensity. Structures in the ion or electron yields as a function of intensity are seldom observed. This does not apply to these nonlinear optical processes, though of course it is much harder to extract the single-atom dynamics because of propagation.

In the last three sections, we present additional experimental results obtained in other conditions. We have varied the focusing geometry, the atomic density in the jet, and the atomic system, in order to test the robustness of the spatial oscillations as a function of Z (an effect due to phase matching) and also of the structures in the intensity dependences (an effect due to the single-atom response).

D. Influence of the focusing conditions

We have performed experiments with a $f = 300$-mm focusing lens, thus doubling the confocal parameter from $b = 1.5$ mm to $b = 3$ mm. Figure 5 shows the results obtained for the 13th harmonic as a function of the position Z of the focus at several intensities. We also observe regular oscillations, with a spatial period equal to 1.1 mm, slightly larger but consistent with the 0.8-mm value for the geometrical coherence length. This confirms that phase matching of the high harmonics in the experimental conditions is limited by focusing and not by other dispersion type of effects.

In Fig. 6, we compare 7th harmonic intensity dependences obtained with the two focusing lenses. The loose focusing configuration enhances the harmonic conversion by about one order of magnitude, owing to the b^3 power law (see [4]). However, the two curves exhibit sudden slope changes at approximately the same intensities. This confirms that these discontinuities are closely linked to microscopic effects occurring at definite intensities.

E. Influence of the atomic density

We compare in Fig. 7 results obtained for the 7th and 13th harmonics as a function of the position of the focus in the jet when the laser is focused at 0.5 mm below the nozzle of the jet, as before, and at 1.5 mm below it. The pressure is estimated to be a factor of 5 lower at 1.5 mm than at 0.5 mm (3 Torr instead of 15 Torr) and the atomic density distribution was checked not to change significantly. The 15-Torr data are shown as solid circles,

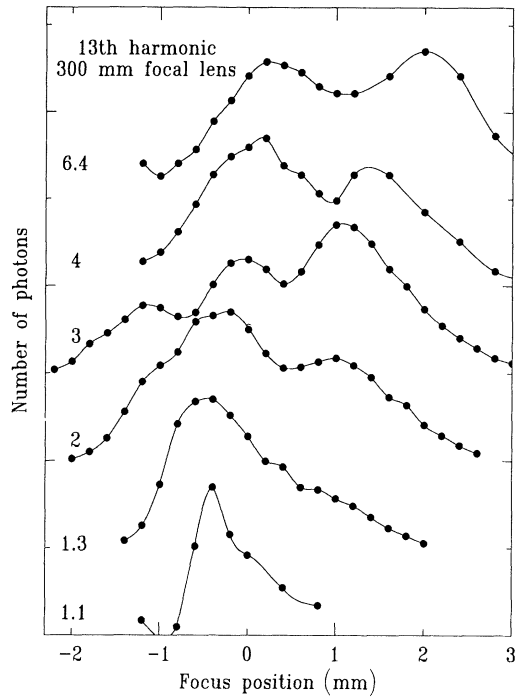

FIG. 5. Number of photons at the 13th harmonic as a function of the position of the focus in the jet. This result is obtained with the f=300-mm lens.

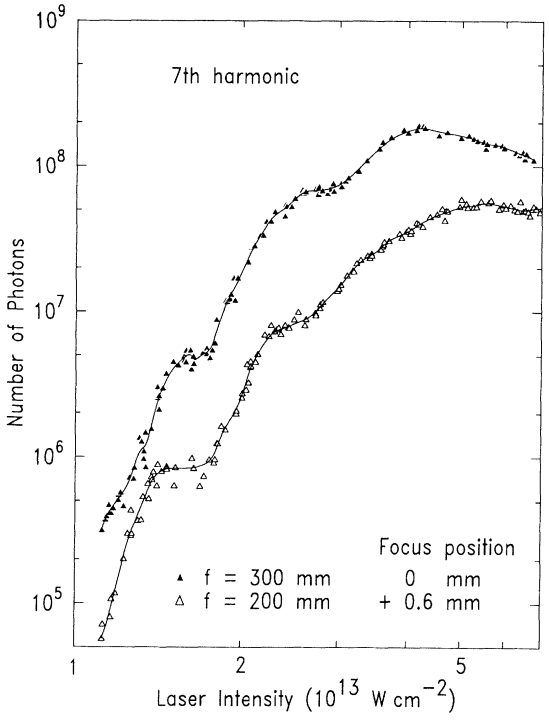

FIG. 6. Number of photons at the 7th harmonic as a function of the laser intensity, with the f = 200- and f=300-mm focal lenses.

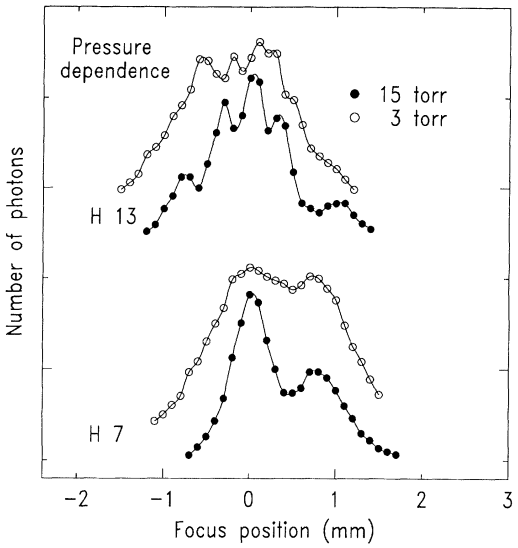

FIG. 7. Number of photons at the 7th and 13th harmonics as a function of Z at 0.5 mm (solid circles) and at 1.5 mm (open circles) from the nozzle of the jet.

while those at 3 Torr arbitrarily placed above the others are indicated by the open circles. This comparison shows that the period of the oscillations along the propagation axis does not depend on pressure. The observed period is therefore mainly due to the focusing geometry.

In Fig. 8, we compare intensity dependences for the 13th harmonic (at $Z = 0$) at different backing pressures: 150, 250, and 350 Torr. The pressure in the jet is expected to follow approximately linearly the backing pressure [27] with here a factor of ten difference. The two structures appear exactly at the same intensities, which again shows that their origin is microscopic. It shows that the structures are pressure independent and can be associated to the single-atom response. However, the behavior in the saturation region does depend on the pressure. Indeed, the free electrons have a deleterious effect on phase matching which increases with the pressure. The results of Fig. 8 show that the saturation of the curves is due to both the depletion of the neutral atoms population and to the effect of the free electrons on phase matching.

F. Influence of the atomic medium

Finally, we have investigated whether these effects were particular to the xenon atom or whether they were also present for other atomic systems. We present in Fig. 9 the variation with intensity of the 9th, 15th, and 17th harmonics generated in argon. We use a 200-mm focal length as before and a slightly higher pressure, 30 Torr. Similar steplike structures as for xenon appear at higher intensities and higher harmonic orders.

Note that we observed generation of the 13th harmonic in argon, in contrast to our earlier measurements [2]. The improved signal-to-noise ratio, due to the slightly higher

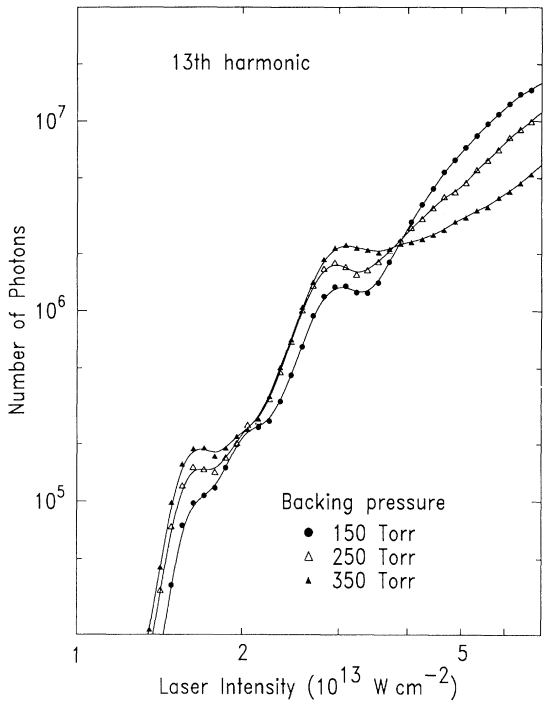

FIG. 8. Number of photons at the 13th harmonic at $Z = 0$ at three different backing pressures: 150, 250, and 350 Torr.

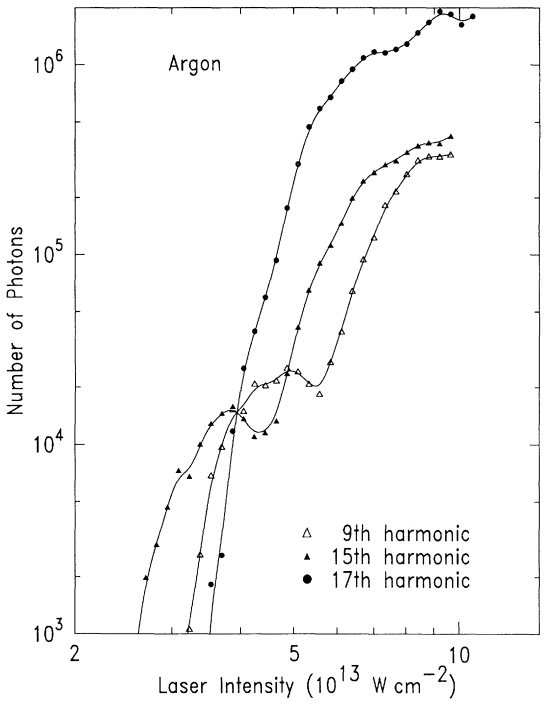

FIG. 9. Number of photons at the 9th, 15th, and 17th harmonics in argon as a function of intensity.

pressure, was sufficient for enabling us to observe barely the 13th harmonic, which lies about one order of magnitude below the others (and below the average level of the plateau). We tested the robustness of the 13th harmonic with the interaction geometry and atomic density and we concluded that the lower yield for the 13th harmonic was not due to absorption or phase-matching effects, but rather to the single-atom response. Miyazaki and Sakai [6] also observed minima in the harmonic intensity distributions for the harmonics close to the ionization threshold.

IV. DISCUSSION

In this section, we comment on the resonantlike structures observed in the harmonic generation rates. Field-induced resonances have been observed in above-threshold-ionization (ATI) experiments with short pulses (see, e.g., [28–30]) at higher laser frequencies (around 600 nm or 300 nm) than that used in the present experiments. It is now well established that atomic levels of atoms irradiated by a strong laser field undergo important ac-Stark shifts, thus coming into resonance with the dressed ground state. This shift is in general equal to the ponderomotive energy, in particular for the high-lying excited states.

Unfortunately, as far as we know, there has been no short-pulse ATI experiments at 1064 nm yet. At this frequency and at the required intensities, the ac-Stark can be as large as 3 times the photon energy in xenon and 5 times the photon energy in argon. This multiplies the number of possible pathways, making any identification of specific resonances hazardous. The ion yields recorded in these conditions (1064 nm, 40 ps) [31] and with shorter pulses (1053 nm, 1 ps) [32, 33] look smooth and can be interpreted using simple tunneling formulas [34].

Results of numerical calculations performed in hydrogen and xenon at 1064 nm [14,20], and obtained by integrating the time-dependent Schrödinger equation (see, for example, Fig. 8 in [20]) and recent Floquet calculations in hydrogen [35], show that the dynamics of harmonic generation processes looks very complicated, with many structures and resonances. These processes probe the part of the wave function that goes back to the ground state and seem to be much more sensitive to the intimate dynamics of the strong-field excitation of an atom than ionization. The latter probes the part of the wave function escaping from the atom, leading to much smoother rates as a function of intensity. At visible and ultraviolet frequencies, the dynamics is somewhat simpler, the atomic levels do not shift as much and resonances in general can be more clearly identified [36, 37]. Here, at 1064 nm, it is much harder to identify a given level shifting in the laser field, because too many pathways interfere.

In addition, phase matching is expected to modify considerably the single-atom picture, and in a nontrivial fashion, in contrast to electron or ion yields measurements. In order to investigate more precisely how phase matching modifies a resonant structure, we have performed model calculations. We have considered sev-

eral resonant profiles as a function of intensity, with various widths and strengths relative to the background, and solved the propagation equation with this profile as a source. The idea is to determine approximately what kind of structures in the single-atom response can survive propagation without being totally washed out and can give steplike broad features similar to those observed in the experiments. More systematic investigations, including calculations using realistic polarization fields obtained by solving the time-dependent Schrödinger equation will be presented in a second article. Our preliminary conclusion is that phase matching does a significant averaging of any variation in the single-atom harmonic generation yield. Any structure must be one or two orders of magnitude high in order to be clearly visible in the propagated results. An example is shown in Fig. 10. In order to model a resonance in, for instance, the 7th harmonic emission rate, we superposed a broad resonance peak, including a π phase slip across the resonance, on a nonresonant background. We use the jet profile determined experimentally. No ionization is considered in this simple model. The propagation equation is then solved numerically, which allows us to take into account the effect of focusing, of atomic dispersion, etc. [20]. The solid line shows the model intensity dependence of the dipole moment $|d_{7\omega}|^2$; the other curves represent the harmonic yields obtained for different focus positions in the jet. The pronounced structure in the single-atom data does indeed lead to steplike features whose importance depends on the geometry. Note that, for some focus positions, the effect of the resonance is almost totally smoothed out. This is completely consistent with the experimental data. Moreover, the change of slopes does not always occur at the peak position but a higher intensity (a delayed effect). This result, combined to the extreme complexity of single-atom responses computed numerically, leads us to believe that any assignment of resonant features to definite levels would be quite speculative.

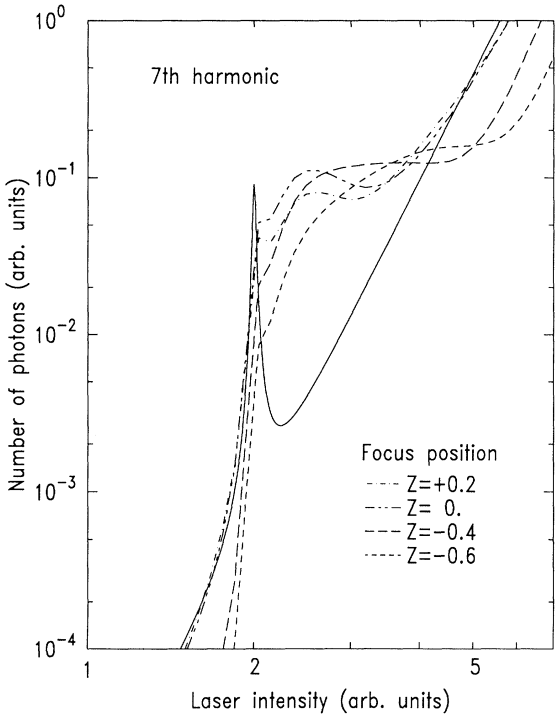

FIG. 10. Intensity dependence of a model 7th harmonic exhibiting a field-induced resonance for different focus positions. The single atom curve is shown as a solid line.

The influence of resonances in the harmonic generation process also allows us to understand why the variation of the number of photons with the focus position depends so strongly on the laser intensity. A resonance in the atomic rate occurs at a given intensity I_R. Atoms located so that the local maximum intensity I_M, obtained at the peak of the pulse, is equal to I_R will have a dominant contribution to the resonant emission. Atoms located closer to the focus, for which $I_M > I_R$, emit resonantly in the leading and falling edges of the pulse, during a much shorter period. Their contribution is expected to be much less important, as well as distributed over a wider spectrum. This results in a complex spatial structure for resonant harmonic generation, comparable to that observed in multiphoton ionization [38] but not identical. In contrast to ionization processes, harmonic generation involves the addition of the amplitudes of the dipoles emitted at various places in the interaction region, with a space-dependent phase relationship. Consider for example what happens on the propagation axis. Resonant emission occurs in two positions symmetric relative to the focus. The effect of the resonance on the total harmonic yield will be enhanced or reduced, depending on whether the wavelets emitted at these two positions add constructively or destructively. This interference depends on the distance between the two positions, relative to the coherence length, and consequently on the laser peak intensity.

V. CONCLUSION

In this work, we have performed systematic studies of harmonic generation processes in xenon using a 1064-nm Nd-YAG laser in the 10^{13} to 5 $\times 10^{13}$ W/cm^2 intensity range. The variation of the harmonic generation yields as a function of the position of the focus in the nonlinear medium has helped in understanding how phase matching of the high harmonics can be accomplished. In a strong-field regime, the fields are constructed through a series of interferences, which can be probed in a tight focusing geometry, by varying the focus position in the jet, provided the latter presents edges. Although the period of the fringes thus obtained is essentially independent of the laser intensity at which the curve is recorded, the overall pattern was found to be strongly intensity dependent. Moreover, the variations of the harmonic generation yields as a function of intensity show structures, which can be either distinct or blurred depending on the beam focus position in the jet. These results, combined with studies of the effect of propagation of model resonances, are interpreted as the signatures of quite accidented single-atom harmonic generation rates. This is consistent with the behaviors of the single-atom har-

monic emission rates [14, 35]. These structures are more or less apparent in the macroscopic yield depending on the phase-matching conditions, i.e., on the exact geometry of the interaction.

APPENDIX A: RECIPROCITY RELATIONS OF HARMONIC GENERATION

The expressions obtained in perturbation theory, as well as some of the numerical results presented in the case of I^p power laws, are symmetric with respect to the center of the jet, whereas the experimental results are clearly asymmetric. It is therefore of interest to investigate what might cause this asymmetry.

The outgoing harmonic field may be written as [19]

$$\mathcal{E}_q(\mathbf{r}') = \left(\frac{q\omega}{c}\right)^2 \int \frac{e^{ik_q|\mathbf{r}'-\mathbf{r}|}}{|\mathbf{r}'-\mathbf{r}|}\mathcal{P}_q(\mathbf{r})\, d^3r. \tag{A1}$$

Let us compare the harmonic fields created far from the medium in two geometries, such that the focus is located at the symmetric positions $+Z$ and $-Z$; the corresponding physical quantities will be denoted by a superscript $+Z$ $(-Z)$. We start from Eq. (A1), written in the paraxial approximation in the form

$$\mathcal{E}_q^{+Z}(r',z') = (q\omega/c)^2 \int d^2r \int_0^{+\infty} dz \left\{ \frac{\mathcal{P}_q^{+Z}(r,z)}{z'-z} \exp\left(i\int_z^{z'} \Delta k(z'')dz''\right) \exp\left(\frac{ik_q[(x'-x)^2+(y'-y)^2]}{2(z'-z)}\right) + \frac{\mathcal{P}_q^{+Z}(r,-z)}{z'+z} \exp\left(i\int_{-z}^{z'} \Delta k(z'')dz''\right) \exp\left(\frac{ik_q[(x'-x)^2+(y'-y)^2]}{2(z'+z)}\right)\right\}. \tag{A2}$$

We assume the following conditions:

$$\rho^{+Z}(z) = \rho^{-Z}(-z), \tag{A3}$$

$$\mathrm{Re}(\Delta k_q^{+Z})(+z) = \mathrm{Re}(\Delta k_q^{-Z})(-z), \tag{A4}$$

$$\mathrm{Im}(\Delta k_q^{\pm Z})(z) = 0 \quad \text{(no absorption)}, \tag{A5}$$

$$\mathrm{Im}(d_q) = 0 \quad \text{(the dipole moment has no intrinsic phase)}. \tag{A6}$$

The phase of the polarization then follows that of the laser field, so that

$$\mathcal{P}_q^{+Z}(r,z) = \mathcal{P}_q^{-Z\,*}(r,-z), \tag{A7}$$

where the asterisk denotes the complex conjugate. One may easily check that, under the assumptions (A3)–(A6),

$$\mathcal{E}_q^{+Z}(r',z') = e^{2ik_q z'}\mathcal{E}_q^{-Z\,*}(r',z') + O(L/z'). \tag{A8}$$

The intensity of the harmonic field, obtained by integrating $|\mathcal{E}_q|^2$, and therefore independent of z' for $z' \gg L$, is identical in both geometries. This might be considered as an example of generalization of the Lorentz reciprocity theorem [39].

Let us analyze these four conditions (A3)–(A6).

Condition (A3) requires the jet profiles ρ^{+Z} and ρ^{-Z} to be symmetric with respect to one another. This is valid, even with ionization, if the initial jet profile itself is symmetric.

Condition (A4) will be fulfilled, even in the case of an intensity-dependent phase mismatch, if condition (A3) already is and if the fundamental field amplitude remains symmetric with respect to the focus. This approximation breaks down if the laser gets significantly defocused owing to a large amount of ionization [20, 40], which is not the case in the intensity and pressure ranges considered here. Wave-coupling effects, expected to be weak in the present experiments, would be another cause for asymmetry, as the other harmonic fields do not present the required symmetries.

Condition (A5) amounts to neglecting reabsorption of the harmonic photons. This is certainly not valid for harmonics with photon energies larger than the atomic ionization energy, but should hold for lower harmonics, at least in a perturbative picture.

Finally, condition (A6) is expected to be true only in a perturbative regime and for the harmonics of the discrete spectrum. Nonperturbative calculations [35, 41] predict that high-order harmonics are no longer in phase with the laser. This effect could be the main cause of asymmetry of the harmonic yields as a function of the position of focus in the medium.

[1] A. McPherson, G. Gibson, H. Jara, U. Johann, T. S. Luk, I. McIntyre, K. Boyer, and C. K. Rhodes, J. Opt. Soc. Am. B **4**, 595 (1987).
[2] X. F. Li, A. L'Huillier, M. Ferray, L. A. Lompré, G. Mainfray, and C. Manus, Phys. Rev. A **39**, 5751 (1989).
[3] A. L'Huillier, L. A. Lompré, G. Mainfray, and C. Manus, in *Atoms in Intense Laser Fields*, edited by M. Gavrila, Advances in Atomic, Molecular and Optical Physics, Suppl. 1 (Academic, New York, 1992), p. 139.
[4] Ph. Balcou, A. S. L. Gomes, C. Cornaggia, L. A. Lompré, and A. L'Huillier, J. Phys. B **25**, 4467 (1992).
[5] N. Sarakura, K. Hata, T. Adachi, R. Nodomi, M. Watan-

abe, and S. Watanabe, Phys. Rev. A **43**, 1669 (1991).
[6] K. Miyazaki and H. Sakai, J. Phys. B **25**, L83 (1992).
[7] J. Reintjes, *Nonlinear Optical Parametric Processes in Liquids and Gases* (Academic, New York, 1984).
[8] J. F. Ward and G. H. C. New, Phys. Rev. **185**, 57 (1969).
[9] A. H. Kung, Opt. Lett. **8**, 24 (1983).
[10] J. Bokor, P. H. Bucksbaum, and R. R. Freeman, Opt. Lett. **8**, 217 (1983).
[11] A. Lago, G. Hilber, and R. Wallenstein, Phys. Rev. A, **36**, 3827 (1987).
[12] A. Lago, G. Hilber, R. Hilbig, and R. Wallenstein, Laser Optoelektr. **17**, 357 (1985).
[13] A. L'Huillier, X. F. Li, and L. A. Lompré, J. Opt. Soc. Am. B **7**, 527 (1990).
[14] J. L. Krause, K. J. Schafer, and K. C. Kulander, Phys. Rev. A **45**, 4998 (1992).
[15] K. C. Kulander and B. W. Shore, Phys. Rev. Lett. **62**, 524 (1989); J. Opt. Soc. Am. B **7**, 502 (1990).
[16] J. H. Eberly, Q. Su, and J. Javanainen, Phys. Rev. Lett. **62**, 881 (1989); J. Opt. Soc. Am. B **6**, 1289 (1989).
[17] R. M. Potvliege and R. Shakeshaft, Phys. Rev. A **40**, 3061 (1989).
[18] G. Bandarage, A. Maquet and J. Cooper, Phys. Rev. A **41**, 1744 (1990).
[19] A. L'Huillier, K. J. Schafer, and K. C. Kulander, Phys. Rev. Lett. **66**, 2200 (1991); J. Phys. B **24**, 3315 (1991).
[20] A. L'Huillier, Ph. Balcou, S. Candel, K. J. Schafer, and K. C. Kulander, Phys. Rev. A **46**, 2778 (1992).
[21] A. L'Huillier, Ph. Balcou, and L. A. Lompré, Phys. Rev. Lett. **68**, 166 (1992)
[22] P. D. Maker, R. W. Terhune, M. Nisenoff, and C. M. Savage, Phys. Rev. Lett. **8**, 21 (1962).
[23] R. Bonifacio and P. Meystre, Opt. Commun. **27**, 147 (1978).
[24] S. W. Allendorf, J. K. Crane, K. S. Budil, and M. D. Perry (unpublished); J. K. Crane *et al.*, *OSA Topical Meeting on Short Wavelength Coherent Radiation* (Optical Society of America, Washington, DC, 1992), Vol. 11.
[25] A. L'Huillier and Ph. Balcou (unpublished).
[26] K. Miyazaki (private communication).
[27] M. D. Perry, C. Darrow, C. Coverdale, and J. K. Crane, Opt. Lett. **17**, 7 (1992); **17**, 523 (1992).
[28] R. R. Freeman, P. H. Bucksbaum, H. Milchberg, S. Darak, D. Schumacher, and M. E. Geusic, Phys. Rev. Lett. **59**, 1092 (1987); R. R. Freeman and P. H. Bucksbaum, J. Phys. B **24**, 325 (1991).
[29] M. D. Perry, A. Szöke, and K. C. Kulander, Phys Rev. Lett. **63**, 1058 (1990).
[30] P. Agostini, P. Breger, A. L'Huillier, H. G. Muller, G. Petite, A. Antonetti, and A. Migus, Phys. Rev. Lett. **63**, 2208 (1989).
[31] A. L'Huillier, L. A. Lompré, G. Mainfray, and C. Manus, J. Phys. B **16**, 1363 (1983).
[32] S. Augst, D. Strickland, D. D. Meyerhofer, S. L. Chin, and J. H. Eberly, Phys. Rev. Lett. **63**, 2212 (1989).
[33] T. Auguste, P. Monot, L. A. Lompré, G. Mainfray, and C. Manus, J. Phys. B **25**, 4181 (1992).
[34] M. V. Amosov, N. B. Delone, and V. P. Krainov, Zh. Eksp. Teor. Fiz. **91**, 2008 (1986) [Sov. Phys. JETP **64**, 1191 (1986)].
[35] R. M. Potvliege and P. H. G. Smith (unpublished).
[36] J. H. Eberly, Q. Su, J. Javanainen, K. C. Kulander, B. W. Shore, and L. Roso-Franco, J. Mod. Phys. **36**, 829 (1989).
[37] H. Xu, X. Tang, and P. Lambropoulos, Phys. Rev. A **46**, 2225 (1992).
[38] T. J. McIlrath, R. R. Freeman, W. E. Cooke, and L. D. van Woerkom, Phys. Rev. A **40**, 2770 (1989).
[39] R. Petit, *Ondes Electromagnétiques en Radioélectricité et en Optique* (Masson, Paris, 1991).
[40] T. Auguste, P. Monot, L.-A. Lompré, G. Mainfray, and C. Manus, Opt. Commun. **89**, 145 (1992).
[41] K. J. Schafer and K. C. Kulander (private communication).